

Exciton Binding Energy of Monolayer WS₂

Bairen Zhu⁺, Xi Chen⁺, Xiaodong Cui^{1,*}

¹*Department of Physics, The University of Hong Kong, Hong Kong, China*

(Dated: March 21, 2014)

The optical properties of monolayer transition metal dichalcogenides (TMDC) feature prominent excitonic natures. Here we report an experimental approach toward measuring the exciton binding energy of monolayer WS₂ with linear differential transmission spectroscopy and two-photon photoluminescence excitation spectroscopy (TP-PLE). TP-PLE measurements show the exciton binding energy of 0.71 ± 0.01 eV around K valley in the Brillouin zone.

PACS numbers: 78.66.-w 73.22.-f 78.20.-e 78.67.Pt

Coulomb interactions are significantly enhanced in low dimensional systems as a result of spatial confinement, and consequently excitons, quasiparticles of electron-hole pairs bounded by Coulomb force play a pronounced role in their optical properties. Intense research efforts have elaborated a few prominent paradigms of the overwhelming excitonic effects in optical aspects in quantum dots and carbon nanotubes where the exciton binding energies are found to be a fraction of their band gaps in these quasi-zero dimensional (0D) and one dimensional (1D) systems. It is also widely accepted that the pronounced excitonic effects extend to atomically thin 2D systems for instance in monolayer transition metal dichalcogenides (TMDC) owing to the reduced dielectric screening and spatial confinement.[1, 2] Monolayer TMDC is an intrinsic 2D crystal consisting of two hexagonal planes of chalcogen atoms and an intermediate hexagonal plane of metal atoms in a prismatic unit cell. Particularly MX₂ (MoS₂, MoSe₂, WS₂ and WSe₂) demonstrates a transition from indirect gap in bulk form to direct gap of visible frequency in monolayers, which is located at K(K') valley of the Brillouin zone.[3–6] The excitonic effect is expected to influence the optical properties of the monolayers in a non-perturbative way. Ab initio calculations give the direct-gap exciton binding energy in the range of 0.5-1eV which is around $1/3 \sim 1/2$ of the corresponding optical direct gap.[1, 2, 7, 8] Experimental evidence of excitonic effects in monolayer TMDC inherits the study on bulk crystals where the binding energy of direct gap excitons around 55meV was identified with modulated absorption/reflection spectroscopy.[9] Such a big exciton binding energy in bulk form guarantees the robust excitonic nature of optical properties in ultrathin counterparts. Furthermore electric gating dependent photoluminescence experiments identify electron(hole)-bounded excitons, so called trions, with a charging energy E_{bX^-} of 18meV and 30meV in monolayer MoS₂ and MoSe₂ respectively.[10, 11] With a simple 2D exciton model, one could estimate the exciton binding energy around 10-fold of the trion binding energy E_{bX^-} , if equal effective electron and hole mass assumed.[12] Nevertheless the direct measurement of exciton binding energy in monolayer TMDC is lacking.

Here we report an unambiguous measurement of the exciton binding energy of monolayer WS₂ through two-photon photoluminescence excitation (TP-PLE) spectroscopy. Two-photon excitation is a third order optical process involving simultaneous absorption of the two photons which follows selection rules different from those in one-photon (linear) process. As a photon has an odd intrinsic parity, in a system with inversion symmetry one- and two-photon transitions are mutually exclusive: one-photon transitions are allowed between states with different parity and two-photon transitions between states with the same parity. In systems without inversion symmetry like monolayer TMDCs described by a point group of D_{3h} symmetry, parity is not a good quantum number and there exist transitions which are both one- and two-photon allowed. Nevertheless the oscillator strengths of exciton states are generally different between one- and two-photon processes. A simplified exciton model could be described as $U_n^l(\rho = r_e - r_h)\phi_c(r_e)\phi_v(r_h)$ where $\phi_c(r_e)(\phi_v(r_h))$ presents the electron (hole) wave function, and U_n^l is the function of relative motion of electron-hole. The optical transition rates for one- and two-photon processes[13]

$$W_{OP} \sim |A|^2 \sum_{c,v} |\langle c | \varepsilon \cdot p | v \rangle|^2 \sum_{c,v} |\langle \phi_c | \phi_v \rangle|^2 \cdot |U_n^l(\rho = 0)|^2 S_{cv}(\hbar\omega)$$

$$W_{TP} \sim |A_1 A_2|^2 \sum_{c,v} |\langle c | \varepsilon \cdot p | v \rangle|^2 \sum_{c,v} |\langle \phi_c | \phi_v \rangle|^2 |\nabla U_n^l(\rho = 0)|^2 S_{cv}(\hbar\omega_1 + \hbar\omega_2)$$

where A denotes the vector potential of the excitation, ε the light polarization unit vector, $\langle c | \varepsilon \cdot p | v \rangle$ the interband matrix elements, $S_{cv}(\hbar\omega)$ the line-shape function of interband exciton. In a 2D system, U_n^l could be described by a solution of 2D Wannier-Mott exciton $U_n^l(\rho, \theta) = \frac{1}{\sqrt{\pi}(n-\frac{1}{2})^{3/2}} \sqrt{\frac{(n-l)!}{(n+l)!}} \left(\frac{2\rho}{n-\frac{1}{2}}\right)^l \exp\left(-\frac{\rho}{n-\frac{1}{2}}\right) L_n^{2l}\left(\frac{2\rho}{n-\frac{1}{2}}\right) \exp(il\theta)$ and the exciton binding energy could be described as $E_n = \frac{Ry^*}{(n-\frac{1}{2})^2}$ where $n=1,2,\dots$ is the principle quantum number, $l=0,1,\dots(n-1)$ is the angular quantum number, and L_{2n}^l is the associate Laguerre polynomial. As the

exciton oscillator strength decays as n^{-3} , only the ground state ($n=1$) and the first two excited states are considered. In a one-photon process, the ground state $1s$ ($n=1, l=0$) dominates; Whereas in a two-photon process the ground state and ns states ($l=0$) are dramatically subsidized owing to $\nabla U_n^l(\rho=0) \approx 0$ and the $2p$ state dominates. Analyzing the difference between one- and two-photon processes would lead to extracting the exciton binding energy of monolayer TMDC.

Monolayer WS_2 was mechanically exfoliated from single crystal WS_2 onto a silicon substrate capped with 300nm oxide. The monolayer was identified with optical microscope and photoluminescence spectroscopy. The samples in differential transmission measurements were made by transferring the monolayer from silicon substrates to freshly cleaved mica substrates as described in Ref[21]. A Xeon-lamp is used as the light source for transmission spectroscopy. The electric gate dependent PL measurements were carried out on monolayer WS_2 on silicon wafers with a 300nm oxide cap layer. The field effect transistor (FET)-like structure was fabricated with standard optical lithography and thermally evaporated Au/Cr pads serve as source and drain electrodes. The heavily doped silicon substrate works as the back gate. The photoluminescence was excited with a 2.331eV laser (532nm) and the power incident on the sample was limited to below 2uW. Two-photon photoluminescence excitation spectroscopy was carried out with a Ti:sapphire oscillator (repetition rate :80MHz, pulse duration: 100fs) and a confocal setup with a 20X achromatic objective. The power incident on the sample was kept at constant of 2mW.

Figure 1a summarizes linear optical measurements of monolayer and multilayer WS_2 . There are distinct peaks in the differential transmission spectra, labeled as “A”, “B” and “C” respectively. Peaks “A” around 2eV and “B” around 2.4eV at room temperature present the excitonic absorptions at the direct gap located at K valley of the Brillouin zones. The separation between “A” and “B” of 0.38eV rising from the splitting of valence band minimum (VBM) due to spin-orbit coupling (SOC) at K(K’) valley is almost constant in all the layers with various thickness, consistent with the PL spectra.[5, 6] It is the direct result of the suppression of interlayer coupling at K(K’) valley owing to the giant SOC and spin-valley coupling in tungsten TMDC with $2H$ stacking order in which each unit layer is a π rotation of its adjacent layers.[5] The peak “C” around 2.8eV was recognized as the excitonic transitions from multiple points near Γ point of the Brillouin zone.[9] Unlike in many semiconductors, the linear absorption spectra of WS_2 display no gap between distinct excitons and the continuum of direct band-to-band transitions. The continuous absorption originates from the strong electron(hole)-phonon coupling in TMDCs and the efficient phonon scattering fills the gap between the ground state excitons and the band-to-band continuum in

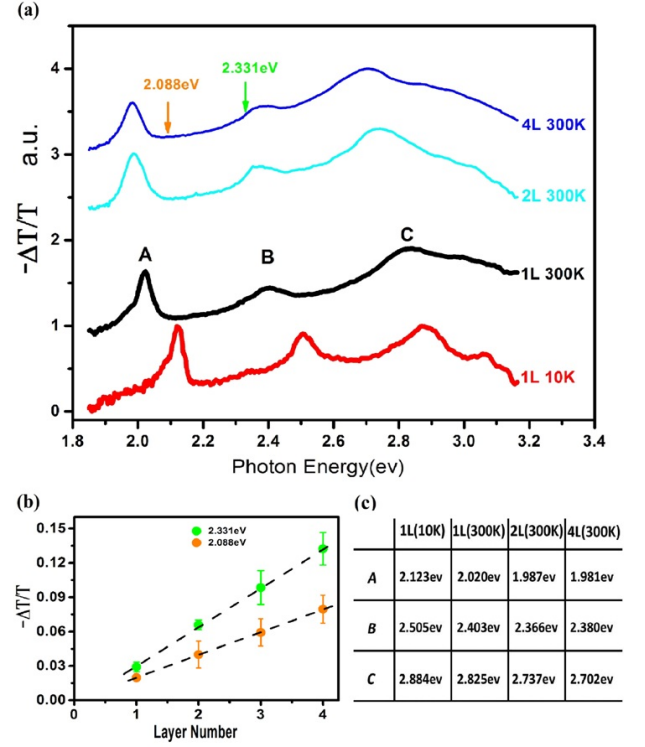


Figure 1: Linear absorption spectra of WS_2 atomically thin films. (a) Normalized differential transmission spectra of multi- and monolayer WS_2 at room temperature and 10K. (b) Absorbance of atomically thin layer at photon energy of 2.088eV (orange) and 2.331eV (green) respectively as indicated by arrows in figure 1(a). The absorbance shows a linearly dependence on layer number, each unit layer with constants of 2.0% and 3.4% respectively. (c) Absorption peak energy values of exciton “A”, “B” and “C”.

the linear absorption spectra.[2] The continuous absorption still survives and no distinct electronic band edge emerges at cryogenic temperature as demonstrated in the differential transmission spectrum measured at 10K. As the temperature drops to 10K, the peak “A” and “B” are both blue-shifted by around 0.1eV and peak “C” is shifted by 0.06eV as shown in Figure 1c. The difference of the energy blue-shift is the direct consequence of the diverse locations of the excitons in the Brillouin zone: exciton “A” and “B” are formed at K valley while “C” is around Γ point. Alternatively a two-photon absorption may be a precise tool to give an indirect measure, which will be presented below.

Figure 1.b shows the absorbance of WS_2 atomically thin films as a function of the thickness above their ground exciton energy, which is approximated with the differential transmission. The absorbance of monolayer and multilayers is linearly proportional to their thickness, each layer absorbing around 2.0% and 3.4% at excitations of 2.088eV and 2.331eV respectively. The high absorbance of monolayer WS_2 comparing with that

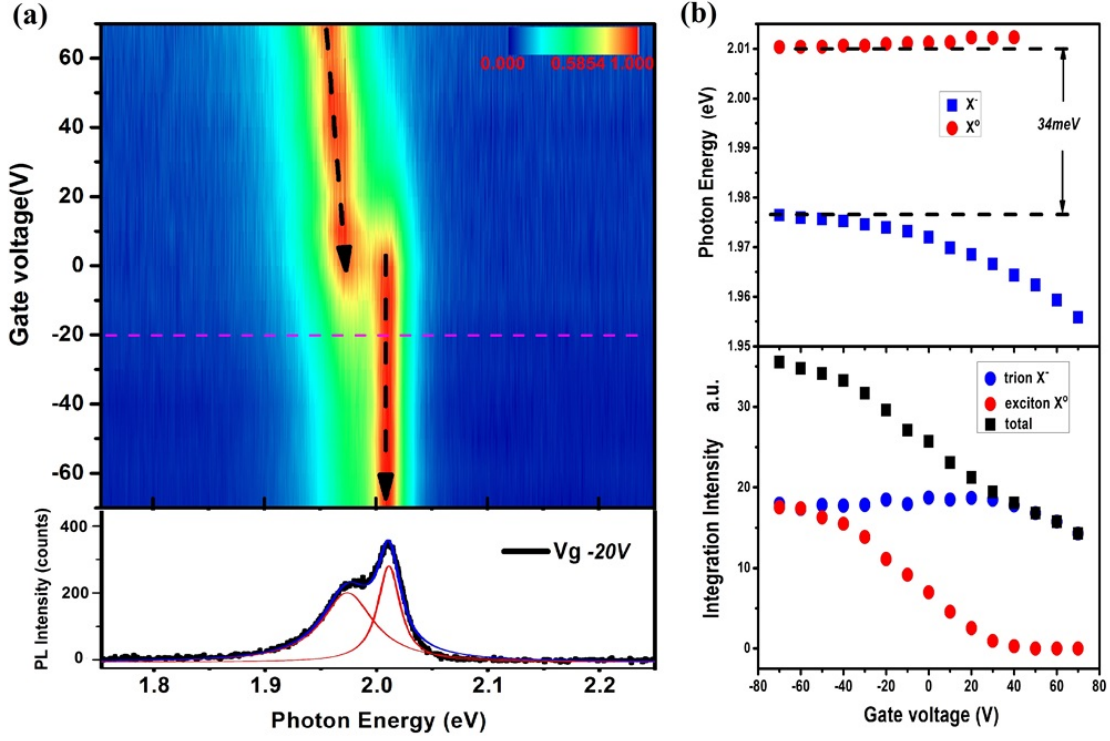


Figure 2: Electric doping dependent photoluminescence spectra at room temperature. (a) Colour contour plot of normalized PL spectra excited by a cw laser (2.331eV) under various back-gate bias. Dashed black arrows contour PL peaks of free exciton and trion states. Even at zero gate bias the trion X^- exists due to defects or substrate interactions. Bottom panel illustrates the PL profile at $V_g = -20V$ (dashed line labelled in the top panel) as a superposition of two Lorentzian shape lines in red. (b) Electric gating dependence of excitons' and trions' energies (upper panel) and the corresponding integrated intensities (bottom panel).

of graphene of 2.3% [14–17] at inter-band transitions originates from two facts: the monolayer WS_2 has a high and similar effective mass in both VBM and CMB, whereas graphene features a massless dispersion. Consequently WS_2 has a higher joint density of states at energy at band-edge interband transitions. Besides the strong exciton effect in WS_2 further enhances the oscillator strength. The linear layer dependence of the absorption gives an experimental evidence of the suppression of interlayer hopping in $2H$ stacked WS_2 as a result of spin-valley coupling.[5, 18] The thickness dependence also could be used as a thickness monitor for multi-layer/monolayer characterization. There is a side bump at the red side of exciton “A”, which modifies the exciton “A” peak away from the symmetric Lorentzian or Gauss line shape. We tentatively attribute the bump to the effect of electron/hole bound exciton or trion.[9, 10] Although the monolayer WS_2 is not intentionally doped, the structural defects and substrate effects such as charge transfer and defects modulate the carrier density away from its insulating state. To confirm the origin of the bump around exciton “A”, we record the photoluminescence (PL) spectra of monolayer WS_2 at various electric gating (from 70V to -70V) which manually tune the Fermi level of

monolayer WS_2 , as show in figure 2a.

There is a significant peak X^- at the red side of the free exciton peak X^0 at zero bias and the PL spectrum could be described by a superposition of two Lorentzian curves which center at peak X^0 and X^- respectively as illustrated in the bottom panel of figure 2a. As the gate voltage goes towards positive values ($V_g > 0$), the free exciton peak X^0 gradually diminishes and totally disappears at $V_g > 40V$. Meanwhile the red-side peak X^- rises to take over the overwhelming weight of the whole PL until it starts to decrease at $V_g > 20$ probably due to the electrostatic screening effect,[19] and the peak X^- is further red-shifted. The electric gating dependence attributes the peak X^- to n-type trion (electron-bounded exciton) states. As V_g goes to negative bias, the free exciton state X^0 takes over the weight of the PL and tends to saturate around $V_g = -70V$. While the trion state X^- monotonically diminishes and the redshift also shows a sign of saturation of -34meV at around $V_g = -70V$. This confirms the trion (electron-bound exciton) origin of the side bump around exciton “A” in the monolayer transmission spectrum, and the trion binding energy of 34meV in monolayer WS_2 . If we follow the simplified trion model in conventional quantum wells[12] and take the effective mass

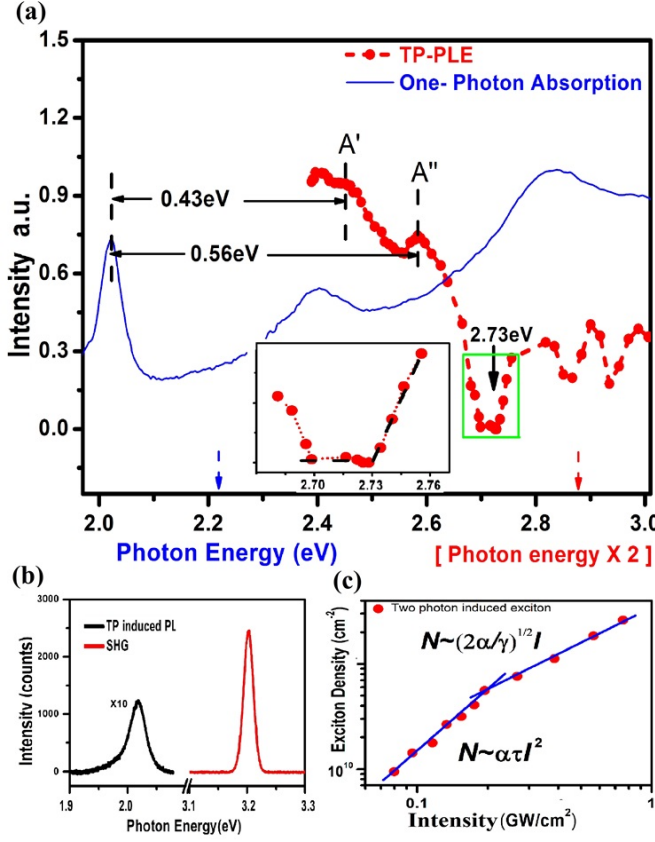


Figure 3: (a) One-photon absorption spectrum (blue) in visible range and two-photon photoluminescence exciton spectrum (red) with the excitation in the range of 1.192~1.5eV where the x axis presents the exciton energy (in blue) for linear absorption and the double of the excitation energy (in red) for TP-PLE. A' and A'' denote the excited states of exciton A and the zoom-in of the gap state section is shown in inset. The TP-PL intensity linearly increases with the excitation energy just above the threshold of the interband continuum, presenting the signature of two-photon process in 2D systems where the polarization sits in the 2D plane. (b) The spectra of two-photon photoluminescence and the second harmonic generation (SHG) at the excitation of 1.6eV. The integrated intensity of the PL is more than one order of magnitude less than that of the SHG. (c) The intensity of two-photon photoluminescence *vs.* the excitation intensity under the excitation at . The fitting lines demonstrate a quadratic- (under low intensity) and a linear-dependence (under high intensity) respectively, which yield the exciton-exciton annihilation rate $\gamma \approx 0.5 \text{ cm}^2/\text{s}$ and the two-photon absorption cross section $\alpha \approx 4 \times 10^4 \text{ cm}^2 \text{ W}^{-2} \text{ S}^{-1}$ at excitation of 1.59eV (780nm).

of either $m_e=0.37$ and $m_h=-0.48$ 20 or $m_e=0.27, m_h=-0.32, 7$ the binding energy of free exciton is estimated at $E_b \approx E_{bX^-} = 0.1 \text{ eV}$.

Figure 3 shows a two-photon photoluminescence excitation (TP-PLE) of monolayer WS_2 , where the PL intensity of free band edge exciton “A” is recorded as a function of the pulsed excitation energy (repetition rate 80MHz, 100femtosecond pulse). Although parity is not a good

quantum number in monolayer WS_2 and one-photon and two-photon optical selection rules are not rigorously exclusive, the oscillator strengths in one-photon and two-photon process have different energy dependence as illustrated above. The TP-PLE displays different features from the linear absorption spectrum, and the TP-PLE and one-photon absorption spectrum offer complementary information on the exciton states. The prominent PL occurs at the excitation around 1.2eV which is the half of the exciton “B” energy and at the excitation around 1.29eV. There is a significant gap state in the range of 1.35~1.36eV, though the PL intensity is not perfectly zero. Upon the excitation just above the gap, the PL intensity shows a linear increase with the excitation energy as shown in the inset. It is the signature of two-photon absorption with in-plane polarization in 2D system.[13] As the excitons “A” and “B” are both from by the spin-split valence bands at K(K') valley with the similar effective mass, a similar strength of binding energy is expected. And if the lower limit of exciton binding energy of 0.5eV is taken,[7] we could attribute the peaks around 2.4eV (2X1.2eV) labeled as “A'” and 2.58eV (2X1.29eV) labeled as “A''” in the TP-PLE spectrum as the excited states of excitons, and the threshold of around 2.73eV to the edge of inter-band continuum. If we assume exciton A and B share the similar strength of exciton binding energy, the peak A' is unlikely to be the excited state of exciton B. We tentatively attribute peak A' and A'' to the 2p and 3p state of exciton “A” respectively. The negligible but nonzero TP-PLE gap states likely result from the re-absorption of the second harmonic excitation, since the SHG intensity is more than one order of magnitude higher than that of two-photon luminescence as shown in Figure 3b. Given that the photoluminescence peaks at 2.02eV presenting the energy of 1s exciton state, the exciton binding energy is extracted from either the energy difference between exciton 1s, 2p and 3p states or the energy difference between exciton 1s and the inter-band continuum. In the former approach, the 2D hydrogenic model gives the energy difference between 1s and 2p(3p) $E_b = 4Ry^* = \frac{9}{8}\Delta E_{1s-2p}$ and $E_b = 4Ry^* = \frac{100}{96}\Delta E_{1s-3p}$ which correspond to $E_b = 0.45 \text{ eV}$ and $E_b = 0.43 \text{ eV}$ respectively. In the later, $E_b = 0.71 \pm 0.01 \text{ eV}$. The difference may lie in the modification of the 2D hydrogenic model by electron-phonon and electron correlation interactions in the monolayer TMDC. Recent first principle simulation shows that the q-dependent screening dramatically enhances the binding energy of the excited states of excitons.[2] If we assume the binding energy of the 2p state is $2/3$ of that of ground state, sharing the similar ratio of monolayer MoS_2 as calculated in Ref.[2], then the exciton binding energy would be incredibly as large as 1.2eV. As the exact ratio of the binding energy 1s *vs.* 2p *vs.* 3p is unknown in addition to the ambiguous state assignments, it is safe to follow the latter approach.

The two-photon absorption has a quadratic depen-

dence on the excitation intensity in principle. The two-photon photoluminescence intensity from monolayer WS_2 displays a clear quadratic dependence on the excitation intensity at low power as shown in figure 3c. As the excitation intensity increases above $0.2\text{GW}/\text{cm}^2$, the PL intensity experiences a clear transition from quadratic to linear dependence on the excitation intensity. If we follow the simple model

$$\frac{dN}{dt} = \alpha I^2 - \frac{N}{\tau} - \frac{1}{2}\gamma N^2 = 0$$

where N denotes the exciton density, I the excitation intensity, α the two-photon absorption cross section, τ the exciton lifetime and γ the exciton-exciton annihilation rate, the fitting of the quadratic dependence $I_{ph} = \alpha\tau I^2$ ($I \rightarrow 0$) gives two-photon absorption cross section of $\alpha \approx 4 \times 10^4 \text{cm}^2 \text{W}^{-2} \text{S}^{-1}$ at 780nm where the PL quantum yield of 4×10^{-3} [3] and the lifetime of exciton of 100ps are assumed. Subsequently the slope of the linear dependence at high intensity $\sqrt{\frac{2\alpha}{\gamma}}$ yields the exciton-exciton annihilation rate $\gamma \approx 0.5 \text{cm}^2/\text{s}$ which is qualitatively consistent with that in monolayer MoSe_2 measured by pump-probe reflection spectroscopy[22]. The linear TP-PL dependence is the evidence of the strong exciton-exciton interactions in monolayer TMDCs.

In summary, we cannot directly identify the electronic interband edge with the linear absorption spectroscopy down to 10K due to the strong electron-phonon scattering and the overlap of excitons around Γ point of the Brillouin zone. The TP-PLE measurements demonstrate a clear electronic interband edge at 2.73eV and the exciton binding energy of $0.71 \pm 0.01\text{eV}$ at monolayer WS_2 . The trion binding energy of 34meV , two-photon absorption cross section $\alpha \approx 4 \times 10^4 \text{cm}^2 \text{W}^{-2} \text{S}^{-1}$ at 780nm and exciton-exciton annihilation rate $\gamma \approx 0.5 \text{cm}^2/\text{s}$ are experimentally obtained. The giant exciton binding energy manifests the unprecedented strong Coulomb interactions in monolayer TMDCs.

- [1] T. Cheiwchanchamnangij and W. R. L. Lambrecht, *Physical Review B* 85, 205302 (2012).
- [2] D. Y. Qiu, F. H. da Jornada, and S. G. Louie, *Physical Review Letters* 111, 216805 (2013).
- [3] K. F. Mak, C. Lee, J. Hone, J. Shan, and T. F. Heinz, *Physical Review Letters* 105, 136805 (2010).
- [4] A. Splendiani, L. Sun, Y. Zhang, T. Li, J. Kim, C.-Y. Chim, G. Galli, and F. Wang, *Nano Letters* 10, 1271 (2010).
- [5] H. Zeng et al., *Sci. Rep.* 3 (2013).
- [6] W. Zhao, Z. Ghorannevis, L. Chu, M. Toh, C. Kloc, P.-H. Tan, and G. Eda, *ACS Nano* 7, 791 (2012).
- [7] H. L. Shi, H. Pan, Y. W. Zhang, and B. I. Yakobson, *Physical Review B* 87 (2013).
- [8] A. Ramasubramaniam, *Physical Review B* 86, 115409 (2012).
- [9] J. Bordas, in *Optical and electrical properties* (Springer, 1976), pp. 145.
- [10] K. F. Mak, K. He, C. Lee, G. H. Lee, J. Hone, T. F. Heinz, and J. Shan, *Nat Mater* 12, 207 (2013).
- [11] J. S. Ross et al., *Nat Commun* 4, 1474 (2013).
- [12] A. Thilagam, *Physical Review B* 55, 7804 (1997).
- [13] A. Shimizu, T. Ogawa, and H. Sakaki, *Physical Review B* 45, 11338 (1992).
- [14] A. Reina, H. Son, L. Jiao, B. Fan, M. S. Dresselhaus, Z. Liu, and J. Kong, *The Journal of Physical Chemistry C* 112, 17741 (2008).
- [15] T. Ando, Y. Zheng, and H. Suzuura, *Journal of the Physical Society of Japan* 71, 1318 (2002).
- [16] K. F. Mak, M. Y. Sfeir, Y. Wu, C. H. Lui, J. A. Misewich, and T. F. Heinz, *Physical review letters* 101, 196405 (2008).
- [17] F. Wang, Y. Zhang, C. Tian, C. Girit, A. Zettl, M. Crommie, and Y. R. Shen, *Science* 320, 206 (2008).
- [18] R. R. Nair, P. Blake, A. N. Grigorenko, K. S. Novoselov, T. J. Booth, T. Stauber, N. M. R. Peres, and A. K. Geim, *Science* 320, 1308 (2008).
- [19] Z. Gong, G.-B. Liu, H. Yu, D. Xiao, X. Cui, X. Xu, and W. Yao, *Nat Commun* 4 (2013).
- [20] S. Tongay et al., *Nano Letters* 13, 2831 (2013).
- [21] D. Xiao, G.-B. Liu, W. Feng, X. Xu, and W. Yao, *Physical Review Letters* 108, 196802 (2012).
- [22] N. Kumar, Q. Cui, F. Ceballos, D. He, Y. Wang and H. Zhao, arXiv:1311.1079

* Electronic address: xdcuiW@hku.hk